DRAG-FREE FLOW OVER A SUBMERGED RANKINE BODY

Julien Dambrine, Evi Noviani, Morgan Pierre

DRAG-FREE FLOW OVER A SUBMERGED RANKINE BODY

JULIEN DAMBRINE, EVI NOVIANI, AND MORGAN PIERRE

Abstract. We prove the existence of a family of immersed obstacles which have zero wave resistance in the context of the two-dimensional Neumann-Kelvin problem. We first build a waveless potential by superposing a source and a sink in a uniform flow, for an appropriate choice of parameters. The obstacle is obtained by a combination of streamlines of the waveless potential. Numerical simulations show that the construction is valid for a large set of parameters.

Keywords: Rankine oval, Neumann-Kelvin problem, wave resistance, potential flow, linear water waves.

1. Introduction

We consider a cylinder at rest, fully immersed in a stream of water of infinite depth. The cylinder is horizontal, infinitely long and oriented orthogonally to the stream, so that the fluid motion is two dimensional. The water is assumed to be homogeneous, inviscid, heavy and incompressible, and the flow is irrotational. At the interface between the water and the air, the waves have a small amplitude and a linearization process can be performed. The potential flow at steady state satisfies a linear boundary value problem known as the Neumann-Kelvin problem.

In this context, for an arbitrary cylinder, the drag (i.e. the horizontal component of the force exerted by the water on the obstacle) is strictly positive in general. This is related to the water/air interface. Indeed, if there were only water, then d'Alembert's paradoxe would assert that the drag is zero. This drag is usually called the *wave resistance* of the obstacle [6, 14].

In this paper, we build a family of obstacles for which the wave-resistance is zero. The idea is to adapt to the 2d Neumann-Kelvin problem the classical construction of Rankine's oval (see e.g. [12]). Namely, we consider a potential flow by adding a source and a sink of same strength in the uniform flow. The source and the sink are positioned horizontally at an arbitrary depth under the water/air interface, and the distance between them is a multiple of the wavelength characteristic of the problem. This construction guarantees that the potential flow is waveless.

Then, we build an obstacle by considering specific streamlines of the potential, namely the two heteroclinic orbits joining the two critical points. The boundary of the obstacle is analytic. The potential outside the obstacle is regular and solves the Neumann-Kelvin problem. Since the potential is waveless, the wave-resistance of the obstacle, which is proportional to the square of the amplitude of the waves far way from the obstacle, is zero. The obstacle is proved to exist if the strength of the source/sink couple is small enough, but numerical simulations show that the construction is valid for a large choice of strengths.

The two-dimensional Neumann-Kelvin (NK) problem has been thoroughly investigated [7]. If the section of the cylinder is a simply connected domain with smooth

boundary, then the NK-problem is uniquely solvable for all values of U_∞ (where U_∞ is the speed of the stream far away in front of the obstacle), except possibly for a finite number of values. If the section is a disk, it is known that the problem is uniquely solvable for all values of U_∞. For an arbitrary section, the unique solvability of the NK-problem for all values of U_∞ is still an open problem. However, Motygin and McIver gave a numerical indication that non-uniqueness holds for certain fully immersed obstacles [11]. McIver [9] also proved the existence of a semi-submerged body for which non-uniqueness holds.

Waveless potentials for the NK-problem have already been a center of interest, especially in the case of semi-submerged obstacles [8]. But up to now, our simple construction adapted from Rankine's oval does not seem to have been pointed out. It solves a shape optimization problem which has been numerically investigated in [13], namely the problem of finding a submerged body with a given area which minimizes the wave resistance. For completeness, let us mention that drag-free bodies have been found for closely related problems [1, 2], by using a different approach.

For an ideal and incompressible fluid whose flow is irrotational, the potential flow is harmonic. Therefore, in order to obtain specific solutions of Euler's equations, building harmonic functions which define simple bodies has long been proved a fruitful idea (see e.g. [10]). For instance, the irrotational flow around a circular cylinder can be found in this way. Rankine's historical idea of using a source in a uniform stream is another example. The term "source" here means the fundamental solution of the problem, also known as the Green's function.

In the case of the Neumann-Kelvin problem, using the Green's function and reformulating the problem in terms of an integral equation involving a distribution of sources on the boundary of the obstacle is one the fundamental ideas which led to proving the unique solvability of the problem [7]. In shape optimization, using the relation between a distribution of sources and the corresponding body is a powerful tool. It has been successfully used in ship design where a Green's function for the 3d Neumann-Kelvin problem is also available (see e.g. [4] and references therein). In a related 2d electromagnetic shaping problem, a striking result states that the distribution of sources exists if and only if the boundary of the body is analytic [5]. Let us mention that for the 3d Neumann-Kelvin problem, we do not expect to find shapes for which the wave resistance is zero, because the wave pattern is more complex. This has been proved rigorously by Krein for the wave resistance of thin ships based on Michell's integral [6].

The paper is organized as follows. We first recall the setting of the Neumann-Kelvin problem and the definition of the wave resistance. Then, we build a waveless potential based on the Green's function and Rankine's idea. In our main result, Theorem 4.1, we show that this waveless potential defines a so-called "Rankine body". For every positive integer p, we thus obtain a two-dimensional continuum of Rankine bodies which have zero wave resistance. Numerical simulations complete the theoretical results.

2. Wave resistance for the Neumann-Kelvin problem

2.1. **The Neumann-Kelvin problem.** We consider a cylinder at rest, fully immersed in a uniform stream of water of infinite depth. The cylinder is horizontal,

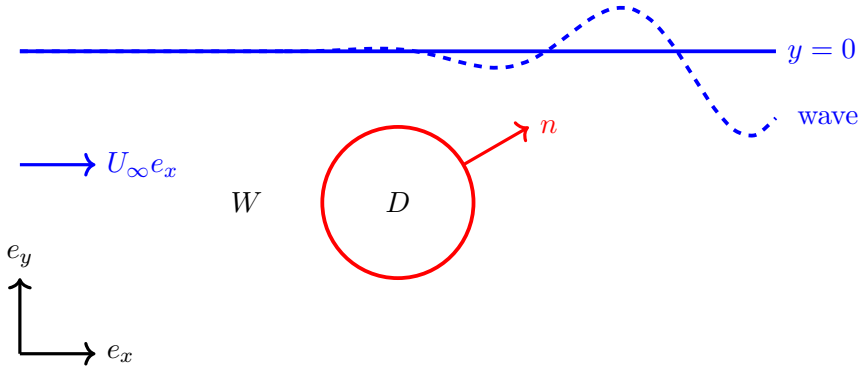

FIGURE 1. Geometrical setting of the problem

infinitely long and oriented orthogonally to the stream, so that the water motion is two dimensional.

We denote $\mathbb{R}^2_-$ the open lower half plan $\mathbb{R} \times (-\infty, 0)$ and (e_x, e_y) the usual orthonormal basis of $\mathbb{R}^2$, with e_y oriented upwards. The cylinder's cross section is represented by a bounded, simply connected domain D of $\mathbb{R}^2_-$ such that $\overline{D} \subset \mathbb{R}^2_-$. The boundary ∂D of D has regularity C^3 at least, and $W = \mathbb{R}^2_- \setminus \overline{D}$ is the cross section of the water domain.

The uniform velocity field is oriented positively in the x direction and given by $U_\infty e_x$ (see Figure 1). It represents the velocity far away from the obstacle. The water is assumed to be a homogeneous, inviscid, heavy and incompressible fluid, and the flow is irrotational, so that the velocity field can be described by the gradient of a potential flow $\Phi(x, y)$. It is assumed that the waves at the free surface have a small amplitude, and it is possible by linearization to transfer the condition on the free surface to the horizontal line $y = 0$.

The boundary value problem which results from the previous assumptions, known as the *Neumann-Kelvin problem*, is the following: find a function $\Phi \in C^2(\overline{W})$ which satisfies

$$\Delta\Phi = 0 \qquad \text{in } W, \tag{2.1}$$

$$\partial^2_{xx}\Phi + \nu\partial_y\Phi = 0 \qquad \text{when } y = 0, \tag{2.2}$$

$$\partial_n\Phi = 0 \qquad \text{on } \partial D, \tag{2.3}$$

$$\sup_W |\nabla\Phi| < +\infty \quad \text{and} \quad |\nabla\Phi - U_\infty e_x| \to 0 \text{ as } x \to -\infty \tag{2.4}$$

In equation (2.2), the positive constant ν, called the *wavenumber*, is related to U_∞ through $\nu = g/U^2$ where g is the standard gravity. In (2.3), $\partial_n\Phi$ denotes the derivative of Φ in the direction n, where n is the outward normal to D.

The unknown function Φ is velocity potential. The Neumann-Kelvin problem is usually expressed in terms of the perturbed potential $\tilde{\Phi} = \Phi - U_\infty x$. We note that a solution of (2.1)-(2.4) may only be defined up to a constant.

Equation (2.1) expresses the conservation of mass. Equation (2.2) can be interpreted as a linearization of the free surface condition, whereas (2.3) is the impermeability condition at the surface of the obstacle. The second condition in (2.4)

says that far away upstream, the velocity field is close to $U_\infty e_x$; it must be satisfied uniformly in y. The first estimate in (2.4) ensures the well-posedness of the Neumann-Kelvin problem, under certain conditions. In a way, it ensures that the potential is physically meaningful.

Far away downstream, the obstacle generates a sinusoidal wave pattern with *wavelength* $\lambda = 2\pi/\nu$. More precisely, we have [7]:

Theorem 2.1. *Let $\Phi \in C^2(\overline{W})$ be a solution of (2.1)-(2.4). Then the following asymptotic formula holds as $|z| \to +\infty$ (where $z = x + iy$):*

$$\Phi(x,y) = U_\infty x + c + \Theta(x,y) + H(x)(\mathcal{A}\sin(\nu x) + \mathcal{B}\cos(\nu x))e^{\nu y}, \tag{2.5}$$

where $\Theta(x,y) = O(|z|^{-1})$, $|\nabla\Theta(x,y)| = O(|z|^{-2})$, c is an arbitrary constant and $\mathcal{A}$, $\mathcal{B}$ are constants which depend only on ν and the values of Φ, $\partial_n\Phi$ on ∂D.

In the statement above, c is an arbitrary constant and H is the Heaviside function defined by $H(x) = 1$ if $x > 0$ and $H(x) = 0$ if $x < 0$. We have set $z = x + iy$ for brevity. The constants $\mathcal{A}$ and $\mathcal{B}$ are proportional to the amplitudes of the sine and cosine waves, respectively, representing the wave pattern at infinity downstream.

The Neumann-Kelvin problem has been thoroughly studied [7]. Concerning uniqueness, it is known that for any $\nu > 0$ with a possible exception of a finite set of values, there is at most one (up to a constant term) solution of (2.1)-(2.4). In the case of a disc, it is known that the Neumann-Kelvin problem has a unique solution for all values of ν. For an arbitrary domain D, the unique solvability of (2.1)-(2.4) for all values of ν remains an open problem.

2.2. **Wave resistance.** With our assumptions, the force exerted by the water on the obstacle is given by

$$F = -\int_{\partial D} p\, n ds,$$

where p is the pressure at the surface of the obstacle. The horizontal component of F is the *drag* and its vertical component is the *lift*. Here, we focus on the drag. If there were no free surface, then F would be zero by d'Alembert's paradoxe. Thus, the presence of a drag in the Neumann-Kelvin model is related to the production of waves behind the obstacle. This drag is usually called the *wave resistance* of the obstacle, and it is equal to

$$R_w = -\int_{\partial D} p\, n \cdot e_x\, ds.$$

From Bernoulli's equation, it follows that

$$R_w = \frac{\rho}{2}\int_{\partial D} |\nabla\Phi|^2 n \cdot e_x\, ds, \tag{2.6}$$

where ρ is the density of the water. Using several integrations by parts on well-chosen paths, the following result can be proved [7, Section 7.3]:

Theorem 2.2. *Let Φ solve (2.1)-(2.4). Then*

$$R_w = \frac{\rho\nu}{4}(\mathcal{A}^2 + \mathcal{B}^2), \tag{2.7}$$

where $\mathcal{A}$ and $\mathcal{B}$ are the coefficients in the asymptotic formula from Theorem 2.1.

This result shows that the wave resistance is proportional to the square of the amplitude of waves downstream, far away from the obstacle.

3. Construction of a waveless Rankine potential

3.1. **Green's function for the Neumann-Kelvin problem.** For every $(x_1, y_1) \in \mathbb{R}^2_-$, we define the function

$$\begin{aligned}\mathcal{G}_{(x_1,y_1)}(x,y) \;:=\; & \frac{1}{2\pi}\log(\nu|z-z_1|) + \frac{1}{2\pi}\log(\nu|z-\bar{z}_1|) - e^{\nu(y+y_1)}\sin(\nu(x-x_1)) \\ & + \frac{1}{\pi}\int_0^{+\infty} \frac{\cos(k(x-x_1))}{k-\nu} e^{k(y+y_1)}dk. \end{aligned} \tag{3.1}$$

As previously, we have set $z = x+iy$ and $z_1 = x_1+iy_1$ for brevity. The integrand is singular at $k=\nu$, so that the integral is understood as the Cauchy principal value.

It is proved in [7] that $\mathcal{G}_{(x_1,y_1)}$ satisfies the following boundary value problem in $\mathbb{R}^2_-$:

$$\Delta \mathcal{G}_{(x_1,y_1)} = \delta_{(x_1,y_1)} \qquad \text{in } \mathbb{R}^2_-, \tag{3.2}$$

$$\partial^2_{xx}\mathcal{G}_{(x_1,y_1)} + \nu\partial_y \mathcal{G}_{(x_1,y_1)} = 0 \qquad \text{when } y=0, \tag{3.3}$$

$$\sup_{(x,y)\in\mathbb{R}^2_-} \left| \nabla[\mathcal{G}_{(x_1,y_1)}(x,y) - \frac{1}{2\pi}\log(\nu|z-z_1|)] \right| < \infty, \tag{3.4}$$

$$\lim_{x\to-\infty} |\nabla \mathcal{G}_{(x_1,y_1)}| = 0, \tag{3.5}$$

where $\delta_{(x_1,y_1)}$ is the Dirac delta function at (x_1,y_1). In particular, the first equation in (3.3) has to be understood in the sense of distributions.

This means that $\mathcal{G}_{(x_1,y_1)}$ is a Green's function for the Neumann-Kelvin problem. Moreover, we have [7]:

Theorem 3.1. *Let $(x_1,y_1) \in \mathbb{R}^2_-$ be given. Then the following asymptotic formula holds as $|z| \to +\infty$:*

$$\mathcal{G}_{(x_1,y_1)}(x,y) = \frac{1}{\pi}\log(\nu|z|) + r(x,y) - 2H(x)e^{\nu(y+y_1)}\sin(\nu(x-x_1)),$$

where $r(x,y) = O(|z|^{-1})$ and $|\nabla r(x,y)| = O(|z|^{-2})$.

3.2. **Source and sink couple.** Following a classical approach, in the spirit of Rankine's oval [12], we can consider the Green's function $\mathcal{G}_{(x_1,y_1)}$ as a source at point (x_1,y_1) for the Neumann-Kelvin problem.

For $a>0$, $d>0$ and $m>0$, we introduce the potential given by

$$\Phi_{a,d,m}(x,y) = m\mathcal{G}_{(-a,-d)}(x,y) - m\mathcal{G}_{(a,-d)} + U_\infty x. \tag{3.6}$$

This potential is the superposition of a source of strength m at $(-a,-d)$, a sink of strength m at $(a,-d)$ and the potential $U_\infty x$ corresponding to a uniform velocity field $U_\infty e_x$.

Let us denote $z_+ = a - id$ and $z_- = -a - id$. By linearity, we deduce from (3.2)-(3.5) that $\Phi_{a,d,m}$ satisfies

$$\Delta\Phi_{a,d,m} = m\delta_{(-a,-d)} - m\delta_{(a,-d)} \text{ in } \mathbb{R}^2_-, \tag{3.7}$$

$$\partial^2_{xx}\Phi_{a,d,m} + \nu\Phi_{a,d,m} = 0 \text{ when } y=0, \tag{3.8}$$

$$\sup_{(x,y)\in\mathbb{R}^2_-} \nabla[\Phi_{a,d,m} - \frac{m}{2\pi}\log(\nu|z-z_-|) + \frac{m}{2\pi}\log(\nu|z-z_+|)] < +\infty, \tag{3.9}$$

$$\lim_{x\to-\infty} |\nabla\Phi_{a,d,m}| = 0. \tag{3.10}$$

Using Theorem 3.1, the asymptotic behaviour of $\Phi_{a,d,m}$ reads

$$\Phi_{a,d,m}(x,y) = U_\infty x + r_{a,d,m}(x,y) - 2mH(x)e^{\nu(y-d)}[\sin(\nu(x+a)) - \sin(\nu(x-a))], \tag{3.11}$$

where $r_{a,d,m}(x,y) = O(|z|^{-1})$ and $|\nabla r_{a,d,m}(x,y)| = O(|z|^{-2})$.

Since

$$\sin(\nu(x+a)) - \sin(\nu(x-a)) = 2\sin(\nu a)\cos(\nu x), \tag{3.12}$$

we see that the amplitude of the waves downstream is proportional to $\sin(\nu a)$. On choosing $a = p\pi/\nu$ for a positive integer p, we obtain a potential $\Phi_{a,d,m}$ for which the amplitude of the waves downstream vanishes. Such a potential $\Phi_{a,d,m}$ is called *waveless* (see e.g. [8]).

If we can show that this waveless potential $\Phi_{a,d,m}$ corresponds to a solution of the Neumann-Kelvin problem (2.1)-(2.4) for a given domain D, then by comparing the asymptotic expressions (3.11) and (2.5), we obtain that the wave resistance R_w of D will be zero, by (2.7). In other words, we want to prove that for some domain D which contains the singularities z_+ and z_-, equation (2.3) is satisfied. Then, by (3.7)-(3.10), the full Neumann-Kelvin problem will be solved.

In the next section, we will prove that such a domain exists for some values of the parameters; a domain obtained in this manner can be seen as a Rankine body for the Neumann-Kelvin problem.

4. Construction of the Rankine body with zero wave resistance

We set $a = p\pi/\nu$ for some positive integer p. From (3.6), (3.1) and (3.12), we find that

$$\begin{aligned}\Phi_{a,d,m}(x,y) &= U_\infty x + \frac{m}{2\pi}\log(\nu|z-z_-|) + \frac{m}{2\pi}\log(\nu|z-\bar{z}_-|)\\ &\quad -\frac{m}{2\pi}\log(\nu|z-z_+|) - \frac{m}{2\pi}\log(\nu|z-\bar{z}_+|)\\ &\quad -\frac{2m}{\pi}\int_{\mathbb{R}_+}\frac{\sin(kx)e^{k(-d+y)}\sin(kp\pi/\nu)}{k-\nu}dk,\end{aligned} \tag{4.1}$$

where $\mathbb{R}_+ := [0,+\infty)$. In particular, since $\sin(kp\pi/\nu) = (-1)^p\sin((k-\nu)p\pi/\nu)$, the integrand is no longer singular.

It will be more convenient to use a normalization. Thus, we consider the potential

$$\tilde{\Phi}_{a,d,m}(x,y) = \frac{2\pi}{m}\Phi_{a,d,m},$$

which reads

$$\begin{aligned}\tilde{\Phi}_{a,d,m}(x,y) &= \frac{x}{b} - \log(\nu|z-z_+|) + \log(\nu|z-z_-|) - \log(\nu|z-\bar{z}_+|)\\ &\quad + \log(\nu|z-\bar{z}_-|) - 4\int_{\mathbb{R}_+}\frac{\sin(kx)e^{k(-d+y)}\sin(kp\pi/\nu)}{k-\nu}dk,\end{aligned} \tag{4.2}$$

where $b = m/(2\pi U_\infty)$ has the same unit (the meter) as a, x and d. The parameter $a = p\pi/\nu$ is the half-length between the source and the sink, and d is the depth of the source/sink couple. We note that the first three terms in the right-hand side of (4.2) define the velocity potential for the classical Rankine oval with sink at z_+ and source at z_- [12] (see figure 2).

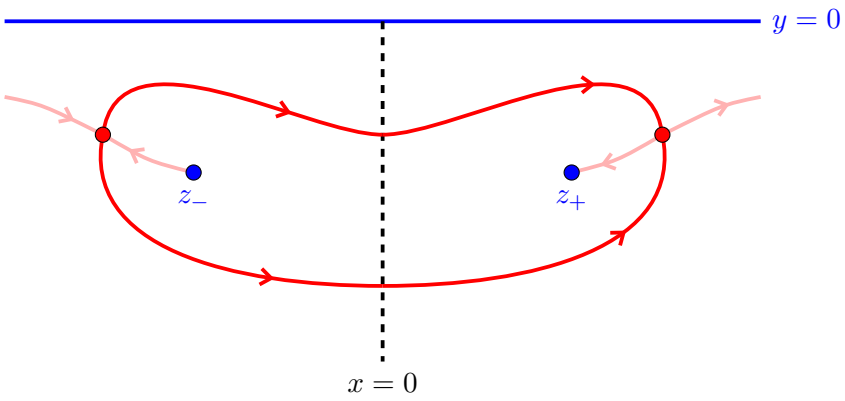

FIGURE 2. Global schematic view of the Rankine body.

The parameter $\nu = g/U_\infty^2 > 0$ is fixed . Thus, the normalized potential $\tilde{\Phi}_{a,d,m}$ only depends on p (through $a = p\pi/\nu$), d and b, and this is also true for $\Phi_{a,d,m}$ as well. We will prove the following

Theorem 4.1. *For every positive integer p and for every depth $d > 0$, there exists $b^\star > 0$ such that for all $b \in (0, b^\star)$, the waveless potential $\Phi_{a,d,m}$ (cf. (4.1)) defines a bounded and simply connected domain $D = \mathcal{R}_{p,d,b}$ with analytic boundary for which the Neumann-Kelvin problem (2.1)-(2.4) is solved. Moreover, this "Rankine body" $\mathcal{R}_{p,d,b}$ contains the singularities and is symmetric about the y axis.*

Remark 4.2. Consider a Rankine body $\mathcal{R}_{p,d,b}$ defined by Theorem 4.1. If the Neumann-Kelvin problem is uniquely solvable for this domain, then the waveless potential $\Phi_{a,d,m}$ is the unique solution. In this case, we can define in a unique way the wave-resistance associated to $\mathcal{R}_{p,d,b}$ (see (2.6)), and this wave resistance is zero by Theorem 2.2. But we do not know whether the Neumann-Kelvin problem is uniquely solvable for the domain $\mathcal{R}_{p,d,b}$ with the specific value ν.

Remark 4.3. The distance between the source and the sink is $2a = 2p\pi/\nu = p\lambda$ where $\lambda = 2\pi/\nu$ is the wavelength characteristic of the Neumann-Kelvin problem, in view of the asymptotic result from Theorem 2.1. This is a simple "necessary" condition for a body to be drag-free.

In the remainder of section 4, for sake of simplicity, we choose $a = \pi/\nu$. We fix an arbitrary depth $d > 0$ for the obstacle. For convenience, we will also write Φ instead of $\tilde{\Phi}_{a,d,m}$.

4.1. **Complex velocity potential and velocity field.** It will prove useful to introduce the complex velocity potential associated to Φ. It reads

$$\begin{aligned}\omega(z) &= \frac{z}{b} - \log(\nu(z - z_+)) + \log(\nu(z - z_-)) - \log(\nu(z - \bar{z}_+)) \\ &\quad + \log(\nu(z - \bar{z}_-)) - 4i \int_{\mathbb{R}_+} \frac{e^{-ikz-kd}\sin(k\pi/\nu)}{k - \nu} dk. \end{aligned} \tag{4.3}$$

Due to the presence of the complex logarithm, this function is well-defined and holomorphic on every simply connected domain included in the set

$$\{z \in \mathbb{C},\ \mathrm{Im}(z) < d/2\} \setminus \{z_+, z_-\}. \tag{4.4}$$

The bound $\mathrm{Im}(z) = y < d/2$ guarantees that the exponential term in the integral term of (4.3) satisfies $|e^{-ikz-kd}| \leq e^{-kd/2}$. Thus, the integral term in (4.3) is holomorphic on $\{z \in \mathbb{C},\ \mathrm{Im}(z) < d/2\}$ (recall that $\sin(k\nu)/(k-\nu)$ is uniformly bounded on $\mathbb{R}$, so that the integral is no longer singular).

The velocity potential Φ and the stream function Ψ are the real and imaginary parts of ω, respectively, i.e.

$$\omega(z) = \Phi(x,y) + i\Psi(x,y). \tag{4.5}$$

As mentioned previously, we choose Φ to be the function defined by (4.2). It is easily seen that Φ is of class C^1 on the set $\mathcal{O}_d \setminus \{z_+, z_-\}$, where

$$\mathcal{O}_d := \{(x,y) \in \mathbb{R}^2,\ y < d/2\},$$

so that by identification, Φ is real analytic on this set. The expression of $\Psi(x,y)$, which depends on the cut chosen for the complex logarithm, will be given later on (see (4.21)).

By differentiating ω with respect to z in (4.5), we obtain the Cauchy-Riemann equations

$$\omega'(z) = \partial_x\Phi(x,y) + i\partial_x\Psi(x,y) = \partial_y\Psi(x,y) - i\partial_y\Phi(x,y), \tag{4.6}$$

which are usually written

$$\begin{cases} \partial_x\Phi = \partial_y\psi, \\ \partial_y\Phi = -\partial_x\psi. \end{cases}$$

In particular, we see that (x,y) is a critical point of Φ (or equivalently, of Ψ) if and only if $z = x + iy$ is a zero of ω'.

Next, by differentiating (4.3) with respect to z, we find that

$$\begin{aligned} \omega'(z) \ &= \ \frac{1}{b} - \frac{1}{z-z_+} + \frac{1}{z-z_-} - \frac{1}{z-\bar{z}_+} \\ &\quad + \frac{1}{z-\bar{z}_-} + 4\int_{\mathbb{R}_+} \frac{ke^{-ikz-kd}\sin(k\pi/\nu)}{k-\nu}dk. \end{aligned} \tag{4.7}$$

We note that $\omega'(z)$ is holomorphic on the set defined by (4.4).

4.2. **Uniqueness of a critical point.** The first step is to find a unique zero of ω' near z_+, for b small enough.

For $z_0 \in \mathbb{C}$ and $r > 0$, we denote $B(z_0, r)$ the open disc of radius r centered at z_0 in $\mathbb{C}$. We have:

Lemma 4.4. *There exist $r_1 > 0$ and $b_1 > 0$ such that for all $b \in (0, b_1)$, there is a unique $z = z(b) \in B(z_+, r_1) \setminus \{z_+\}$ which satisfies $\omega'(z) = 0$. Moreover, z depends analytically on b and $z(b) - z_+ = b + O(b^2)$ as b tends to 0. Finally, $\omega''(z(b)) \neq 0$ for all $b \in (0, b_1)$.*

Proof. From (4.7), it is clear that

$$\omega'(z) = \frac{1}{b} - \frac{1}{z-z_+} + H(z), \tag{4.8}$$

where H is a holomorphic function of z in the neighbourhood of z_+. Thus, for $z \neq z_+$, the equation $\omega'(z) = 0$ is equivalent to

$$b = \frac{z - z_+}{1 - (z-z_+)H(z)}, \tag{4.9}$$

in a neighbourhood of z_+. The derivative of the right-hand side of (4.9) with respect to z at $z = z_+$ is 1, so that we may apply the implicit function theorem, which proves the first part of the claim. The derivative of $z(b)$ at $b = 0$ is obtained on differentiating (4.9) with respect to b, and we find that $z'(0) = 1$, so that $z(b) - z_+ = b + O(b^2)$. Finally, we differentiate (4.8) with respect to z. This yields

$$\omega''(z) = \frac{1}{(z - z_+)^2} + H'(z),$$

which is equivalent to

$$(z - z_+)^2 \omega''(z) = 1 + (z - z_+)^2 H'(z), \tag{4.10}$$

for z near z_+, $z \neq z_+$. By continuity, the right-hand side of (4.10) does not vanish in a neighbourhood of z_+. Thus, by choosing r_1 smaller if necessary (and b_1 accordingly), we can guarantee that $\omega''(z) \neq 0$ on $B(z_+, r_1) \setminus \{z_+\}$. This concludes the proof. □

The following estimate will prove useful.

Lemma 4.5. *For all $z \in \mathbb{C}$ such that $\mathrm{Im}(z) \leq 0$, we have*

$$\left| 4 \int_{\mathbb{R}_+} \frac{k e^{-ikz - kd} \sin(k\pi/\nu)}{k - \nu} dk \right| \leq \frac{C_{num}}{\nu^2 d^3}, \tag{4.11}$$

where C_{num} is a positive real number (independent of ν, d and b).

Proof. We have $\sin(k\pi/\nu) = -\sin((k - \nu)\pi/\nu)$, so that

$$\left| \frac{\sin(k\pi/\nu)}{k - \nu} \right| = \frac{\pi}{\nu} |\operatorname{sinc}((k - \nu)\pi/\nu)|,$$

where sinc is the sine cardinal function. The sinc function is real analytic on $\mathbb{R}$, and its first derivative is uniformly bounded on $\mathbb{R}$ by a numerical constant C_1, so that by the mean value theorem,

$$|\operatorname{sinc}((k - \nu)\pi/\nu)| = |\operatorname{sinc}((k - \nu)\pi/\nu) - \operatorname{sinc}(-\nu\pi/\nu)| \leq C_1 \frac{k\pi}{\nu},$$

for all $k \in \mathbb{R}_+$. Thus,

$$\left| 4 \int_{\mathbb{R}_+} \frac{k e^{-ikz - kd} \sin(k\pi/\nu)}{k - \nu} dk \right| \leq 4 C_1 \left(\frac{\pi}{\nu} \right)^2 \int_{\mathbb{R}_+} k^2 e^{-kd} dk,$$

for all $z \in \mathbb{C}$ such that $\mathrm{Im}(z) \leq 0$. Two integration by parts show that the integral in the right-hand side above is equal to $2/d^3$, so that (4.11) is true with $C_{num} = 8 C_1 \pi^2$. □

Next, we show that for b small enough, ω' does not vanish outside a neighbourhood of $\{z_+, z_-\}$. By symmetry of the velocity field (see (4.17)), we can restrict the study to the open quadrant

$$Q_+ = (0, +\infty) \times (-\infty, 0).$$

The closure of Q_+, $\mathbb{R}_+ \times \mathbb{R}_-$, is denoted $\overline{Q}_+$.

Lemma 4.6. *For all $z \in \overline{Q}_+ \setminus B(z_+, 2b)$, we have*

$$|\omega'(z)| \geq \frac{1}{2b} - \frac{1}{a} - \frac{2}{d} - \frac{C_{num}}{\nu^2 d^3}, \tag{4.12}$$

where C_{num} is the constant in (4.11)*. In particular, for b small enough, we have*

$$|\omega'(z)| \geq \frac{1}{4b}, \quad z \in \overline{Q}_+ \setminus B(z_+, 2b).$$

Proof. For $z \in \overline{Q}_+ \setminus B(z_+, 2b)$, we have

$$|z - z_+| \geq 2b, \quad |z - z_-| \geq a, \quad |z - \bar{z}_+| \geq d \quad \text{and } |z - \bar{z}_-| \geq d.$$

Estimate (4.12) follows from (4.7), (4.11) and the triangle inequality, □

By Lemma 4.4, we can choose $b^\star > 0$ such that $b^\star < b_1$, $2b^\star < r_1$ and $|z(b) - z_+| < 2b$ for all $b \in (0, b^\star)$. With this choice, there is a unique zero of ω' in $B(z_+, 2b^\star) \setminus \{z_+\}$ for every $b \in (0, b^\star)$, namely $z(b)$. By choosing a smaller $b^\star$ if necessary, Lemma 4.6 guarantees that for all $b \in (0, b^\star)$, $z(b)$ is in fact the unique zero of ω' in $\overline{Q}_+ \setminus \{z_+\}$.

For later purpose, we also assume that

$$\frac{d}{8b} > 4\pi \quad \text{and} \quad \frac{d}{8b} > \frac{2C_{num}}{\nu^2 d^3}. \tag{4.13}$$

4.3. **Analysis of the velocity flow.** In this section, we fix a value $b \in (0, b^\star)$ where $b^\star$ is chosen as explained in previously, in Section 4.2. In particular, ω' has a unique zero $z(b) = z_b$ in $\overline{Q}_+ \setminus \{z_+\}$, which belongs to $B(z_+, 2b)$.

The velocity field on

$$\Omega := \mathbb{R}^2_- \setminus \{z_+, z_-\} \tag{4.14}$$

is defined by $\nabla\Phi$. Using (4.7) and the Cauchy-Riemann equations (4.6), we find that

$$\begin{aligned} \partial_x\Phi(x,y) &= \frac{1}{b} - \frac{x-a}{(x-a)^2+(y+d)^2} + \frac{x+a}{(x+a)^2+(y+d)^2} - \frac{x-a}{(x-a)^2+(y-d)^2} \\ &\quad + \frac{x+a}{(x+a)^2+(y-d)^2} - 4\int_{\mathbb{R}_+} \frac{k\cos(kx)e^{k(y-d)}\sin(k\pi/\nu)}{k-\nu}dk, \end{aligned} \tag{4.15}$$

and

$$\begin{aligned} \partial_y\Phi(x,y) &= -\frac{y+d}{(x-a)^2+(y+d)^2} + \frac{y+d}{(x+a)^2+(y+d)^2} - \frac{y-d}{(x-a)^2+(y-d)^2} \\ &\quad + \frac{y-d}{(x+a)^2+(y-d)^2} - 4\int_{\mathbb{R}_+} \frac{k\sin(kx)e^{k(y-d)}\sin(k\pi/\nu)}{k-\nu}dk. \end{aligned} \tag{4.16}$$

It is readily seen that this velocity field satisfies the following symmetry:

$$\partial_x\Phi(-x,y) = \partial_x\Phi(x,y) \quad \text{and} \quad \partial_y\Phi(-x,y) = -\partial_y\Phi(x,y), \quad (x,y) \in \Omega. \tag{4.17}$$

We first notice the following local result:

Proposition 4.7. *The unique critical point z_b of Φ in $\overline{Q}_+ \setminus \{z_+\}$ is a non-degenerate saddle point.*

Proof. On writing the Cauchy-Riemann equations for ω'', in a way analogous to (4.6), we find that

$$\omega''(x+iy) = \partial^2_{xx}\Phi(x,y) - i\partial^2_{xy}\Phi(x,y).$$

Lemma 4.4 asserts that $\omega''(z_b) \neq 0$, that is

$$|\omega''(z_b)|^2 = (\partial^2_{xx}\Phi(x_b,y_b))^2 + (\partial^2_{xy}\Phi(x_b,y_b))^2 > 0, \tag{4.18}$$

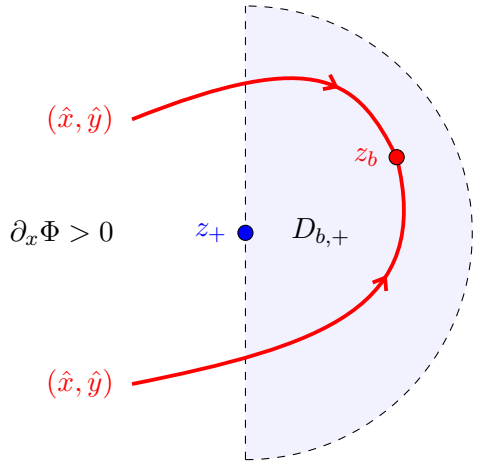

FIGURE 3. Schematic view of the flow near a stop point z_b

where $z_b = x_b + iy_b$. The hessian of Φ at (x_b, y_b) is given by

$$H_b = \begin{pmatrix} \partial^2_{xx}\Phi & \partial^2_{xy}\Phi \\ \partial^2_{xy}\Phi & \partial^2_{yy}\Phi \end{pmatrix},$$

where the partial derivatives are evaluated at (x_b, y_b). The real valued 2×2 matrix H_b is symmetric so it has real eigenvalues λ_1, λ_2. By construction, Φ is harmonic on Ω, i.e. $\Delta\Phi = 0$ in Ω, which yields

$$\partial^2_{yy}\Phi(x_b, y_b) = -\partial^2_{xx}\Phi(x_b, y_b).$$

Thus, the determinant of H_b is

$$\det(H_b) = -|\omega''(z_b)|^2 = \lambda_1\lambda_2 < 0$$

by (4.18). The critical point is therefore a non-degenerate saddle point, as claimed. □

Proposition 4.7 describes the local behaviour of the velocity flow near z_b (see figure 3). Next, we need to use global arguments. For this purpose, we consider the open half-disc

$$D_{b,+} := \{z \in B(z_+, 2b),\ \mathrm{Re}(z) > a\},$$

and we first notice:

Lemma 4.8. *The horizontal component of the velocity field satisfies $\partial_x\Phi \geq 1/(4b)$ on the set $\overline{Q}_+ \setminus (D_{b,+} \cup \{z_+\})$. In particular, z_b belongs to $D_{b,+}$.*

Proof. We argue as in the proof of Lemma 4.6, using a triangle inequality where the term $1/b$ is dominant. Since $|Re(w)| \leq |w|$ holds true for any complex number w, we may estimate the real part of every term in the right-hand side of (4.7) as in Lemma 4.6, and we find that

$$\mathrm{Re}(\omega'(z)) \geq \frac{1}{2b} - \frac{1}{a} - \frac{2}{d} - \frac{C_{num}}{\nu^2 d^3} \tag{4.19}$$

(compare with (4.12)). The only difference happens when $\mathrm{Re}(z) \leq a$ in the term

$$\mathrm{Re}\left(-\frac{1}{z - z_+}\right) = -\frac{x - a}{|z - z_+|^2},$$

which is the second term in the right-hand side of (4.15). But when $x \leq a$, this terms contributes positively to $\partial_x \Phi(x,y)$, so that (4.19) is also true in this case. The smallness assumption on b ensures that $\mathrm{Re}(\omega'(z) \geq 1/(4b)$ in the set under consideration. □

As $\varepsilon \to 0$, we have $\Phi \to +\infty$ on the circle $\partial B(z_+, \varepsilon)$ centered at z_+ with radius ε, because the $-\log \varepsilon$ is dominant in (4.2). In the following, we set $\varepsilon = \varepsilon_b \in (0, b/2)$ small enough so that

$$\Phi(z) > \Phi(z_b) \text{ on } \partial B(z_+, \varepsilon). \tag{4.20}$$

A *trajectory* (x,y) of the velocity field is a maximal solution of the ODE

$$(x(t), y(t)) = \nabla \Phi(x(t), y(t))$$

with values in the open set Ω (cf. (4.14)) By linearization at $z_b = x_b + iy_b$, we deduce from Proposition 4.7 that there are exactly two trajectories arriving at z_b and two trajectories departing from z_b. We have:

Proposition 4.9. *Let $(\hat{x}, \hat{y})$ by either one of the two trajectories arriving at (x_b, y_b). If $(\hat{x}, \hat{y})$ does not reach the axis $x = 0$, then $(\hat{x}, \hat{y})$ stays in the compact set $([0, a + 4b] \times [-4d, -d/4]) \setminus B(z_+, \varepsilon)$.*

Proof. We use the stream function $\psi(x,y) = Im(\omega(z))$ (cf. (4.5)). A determination of ψ on the open set

$$\mathcal{O}_d \setminus (\{(-a, y),\ y < d/2\} \cup \{(a, y),\ y < d/2\})$$

is given by

$$\begin{aligned} \psi(x,y) \quad = \quad & \frac{y}{b} - \arctan\left(\frac{y+d}{x-a}\right) + \arctan\left(\frac{y+d}{x+a}\right) - \arctan\left(\frac{y-d}{x-a}\right) \\ & + \arctan\left(\frac{y-d}{x+a}\right) + 4\int_{\mathbb{R}_+} \frac{\cos(kx) e^{k(y-d)} \sin(k\pi/\nu)}{k-\nu} dk. \end{aligned} \tag{4.21}$$

It is readily seen that ψ can be extended by continuity to a function ψ_1 on the open set

$$\mathcal{O}_{d,1} := \mathcal{O}_d \setminus (\{(a, y),\ y \leq -d\} \cup \{(a, y),\ y \leq -d\}). \tag{4.22}$$

Namely, we can take the sum of the four arctan terms equal to 0 for $x = \pm a$ and $-d < y < d/2$. This amounts to choosing a determination of the complex logarithm in $\omega(z)$, so that ψ_1 is actually analytic on the set $\mathcal{O}_{d,1}$.

Let us now consider the trajectory (x_1, y_1) starting at $(0, -d/2)$. By the Cauchy-Riemann equations, the stream function ψ_1 is constant along this trajectory, as long as this curve stays in $\mathcal{O}_{d,1}$. When y goes from $-d/2$ to $-d/4$ or $-3d/4$, then the difference in the term y/b is equal to $\pm d/(4b)$. In comparaison, the perturbation due to the four arctan terms in (4.21) cannot exceed $\pm 2\pi$, and the perturbation due to the integral term cannot exceed $C_{num}/(\nu^2 d^3)$ (cf. (4.11)). Therefore, by the smallness assumption on b (see (4.13)), the trajectory (x_1, y_1) cannot cross the horizontal lines $y = -d/(4b)$ or $y = -3d/(4b)$. By Lemma 4.8, this means that (x_1, y_1) goes from $(-\infty, y_1^\star)$ to $(+\infty, y_1^\star)$ for some $y_1^\star \in (-d/(4b), 3d/(4b))$.

Since two different trajectories do not cross, this implies that $(\hat{x}, \hat{y})$ does not cross the orbit of (x_1, y_1) and therefore stays below the horizontal line $y = -d/4$

By arguing similarly with another continuous extension of ψ, we see that the trajectory (x_2, y_2) starting at $(0, -3d)$ stays between the horizontal lines $y = -2d$

and $y = -4d$ and goes from $x = -\infty$ to $x = +\infty$. As a consequence, $(\hat{x}, \hat{y})$ stays above the horizontal line $y = -4d$.

Next, we note that $(\hat{x}, \hat{y})$ cannot come from the line $x = a+4b$, otherwise at the last time $\bar{t}$ at which this happens, we would have $\hat{x}'(\bar{t}) \leq 0$ because $x_b = \hat{x}(+\infty) \leq a+2b$, contradicting Lemma 4.8.

Finally, we note that $\Phi(\hat{x}(t), \hat{y}(t))$ is strictly increasing along with time, since

$$\frac{d}{dt}\left[\Phi(\hat{x}(t), \hat{y}(t))\right] = (\hat{x}'(t))^2 + (\hat{y}'(t))^2 > 0. \tag{4.23}$$

Thus, by (4.20), the trajectory $(\hat{x}, \hat{y})$ arriving at z_b cannot come from $\partial B(z_+, \varepsilon)$. This completes the proof. □

We are now in position to prove Theorem 4.1.

Proof of Theorem 4.1. Let $(\hat{x}, \hat{y})$ be either one of the two trajectories arriving at z_b. If this trajectory crosses the vertical axis $x = 0$, then by symmetry of the velocity field, $(\hat{x}, \hat{y})$ is defined for all times and its orbit is a heteroclinic orbit joining the two critical points $(-x_b, y_b)$ and (x_b, y_b). This is what we need.

Assume now by contradiction that $(\hat{x}, \hat{y})$ does not cross the axis $x = 0$. Then by Proposition 4.9, this trajectory stays in a compact subset of Ω. In particular, it is defined for all times and we may consider its α-limit set, namely

$$\alpha(\hat{x}, \hat{y}) := \left\{(x^\star, y^\star) \in \Omega, \text{ s. t. } \exists t_n \to -\infty, \ (\hat{x}(t_n), \hat{y}(t_n)) \to (x^\star, y^\star)\right\}.$$

By definition, the velocity field is the gradient flow of Φ, so that standard arguments (see e.g. [3, Proposition 2.2.2]) show that $\alpha(\hat{x}, \hat{y})$ is a compact and connected set included in the set of critical points of Φ. By Proposition 4.9 and the uniqueness of the critical point in $\overline{Q}_+ \setminus \{z_+\}$, we find that $\alpha(\hat{x}, \hat{y}) = (x_b, y_b)$, which implies that $(\hat{x}(t), \hat{y}(t)) \to (x_b, y_b)$ as $t \to -\infty$. But we know by (4.23) that Φ is strictly increasing along a trajectory. Thus $(\hat{x}, \hat{y})$ cannot come from z_b and arrive at the same point z_b, yielding the contradiction.

This construction gives us two heteroclinic orbits $\hat{\gamma}_+$ and $\hat{\gamma}_-$ joining the points $z_{b,-} := -x_b + iy_b$ and $z_b = x_b + iy_b$. We consider the curve Γ in Ω defined as the union of $\hat{\gamma}_+$, $\hat{\gamma}_-$, z_b and $z_{b,-}$. The stream function is locally constant on $\hat{\gamma}_\pm$, so by the implicit function theorem, $\hat{\gamma}_1$ and $\hat{\gamma}_2$ are analytic curves. By Proposition 4.7 and the Morse lemma, the union of $\hat{\gamma}_1$, $\hat{\gamma}_2$ and z_b is analytic near z_b. A similar statement holds near $z_{b,-}$, so the whole curve Γ is analytic. The Jordan curve theorem shows that the interior of Γ defines a simply connected domain $\mathcal{R}_{d,b}$, which is below the horizontal line $y = -d/4$.

It remains to show that $\mathcal{R}_{d,b}$ contains the singularities z_+ and z_-. By continuity, there is a last time at which the trajectory $(\hat{x}_+, \hat{y}_+)$ with orbit $\hat{\gamma}_+$ reaches the vertical line $x = +a$, say at point $(a, y_{a,+})$. Moreover, by Lemma 4.8, this trajectory has never crossed the vertical line $x = +a$ before. The same holds for the orbit $\hat{\gamma}_-$ which reaches the line $x = +a$ only once, at point $(a, y_{a,-})$. We may assume, by changing the roles of the orbits if necessary, that $y_{a,+} > y_{a,-}$.

Assume by contradiction that $y_{a,-} > -d$. Then $\mathcal{R}_{d,b}$ does not contain the singularity z_+, nor the singularity z_- (by symmetry). From what precedes, we also know that $\hat{\gamma}_\pm$ never cross the vertical lines $\{(\pm a, y), \ y \leq -d\}$. Thus, these orbits belong to the open set $\mathcal{O}_{d,1}$ defined by (4.22). By choosing the continuous extension ψ_1 of ψ on $\mathcal{O}_{d,1}$ as in the proof of Proposition 4.9, we see that ψ_1 is constant on Γ, and

continuous on $\overline{\mathcal{R}}_{d,b}$. Since ψ is harmonic on $\mathcal{R}_{d,b}$ (being the imaginary part of a holomorphic function), this implies by the maximum principle that ψ is constant on $\mathcal{R}_{d,b}$, yielding a contradiction with the uniqueness of the critical point.

If $y_{a,+} < -d$, we also obtain a contradiction, by using a similar argument with another appropriate extension of ψ. This shows that $y_{a,-} < -d < y_{a,+}$, and so $\mathcal{R}_{d,b}$ contains z_+ (and also z_-, by symmetry). The proof is complete. □

5. Numerical simulations

The theoretical construction of our "Rankine bodies" from previous section can easily be applied to obtain numerical simulations. We first give some details on the numerical methods, before discussing the results. The simulations were made with the `Matlab`® software.

5.1. **Numerical methods.**

The central idea for the numerical simulations is to use the complex velocity potential $\omega(z)$ (4.3). The appropriate streamline will give us the Rankine body.

A major difficulty is to compute the integral term, so that we turn back to the Green's function (3.1) for the Neumann-Kelvin problem, and we express its integral term with the help of the exponential integral function. A numerical approximation of this function is available in `Matlab`®.

The exponential integral function is defined for every $w \in \mathbb{C} \setminus \mathbb{R}_-$ by

$$E_1(w) := \int_{w+\mathbb{R}_+} \frac{e^{-z}}{z} dz = e^{-w} \int_0^{+\infty} \frac{e^{-t}}{w+t} dt. \tag{5.1}$$

This function is holomorphic on $\mathbb{C} \setminus \mathbb{R}_-$ and $E_1'(w) = e^{-w}/w$. Thus, $\mathbb{R}_-$ is a branch cut for the antiderivative E_1 of e^{-z}/z.

Let us first consider the integral term in the Green's function (3.1). For (x_1, y_1) and (x, y) in $\mathbb{R}^2_-$, we have as a consequence of the residue theorem [7],

$$\begin{aligned} &\int_0^{+\infty} \frac{\cos(k(x-x_1))}{k-\nu} e^{k(y+y_1)} dk + \pi e^{\nu(y+y_1)} \sin(\nu(x-x_1)) \\ &= \mathrm{Re} \int_{l_-} \frac{e^{-ik(z-\bar{z}_1)}}{k-\nu} dk. \end{aligned} \tag{5.2}$$

Here, l_- is the path of integration going along the positive real k axis and indented below at $k = \nu$. It should be interpreted as the limit

$$\int_{l_-} \frac{e^{-ik(z-\bar{z}_1)}}{k-\nu} dk := \lim_{\varepsilon \to 0^+} \int_{l_\varepsilon^-} \frac{e^{-ik(z-\bar{z}_1)}}{k-\nu} dk,$$

where l_{ε^-} is the path of integration represented in Figure 4.

Next, we set $w_1 = z - \bar{z}_1$ and we consider the path P_- which is built from $P = \{iw_1(k-\nu); k \in \mathbb{R}^+\}$, and avoids the singularity (at 0) from below by a limiting process, as for l_-. We have

$$\int_{P_-} \frac{e^{-z}}{z}\, dz = \int_{l_-} \frac{e^{-iw_1(k-\nu)}}{iw_1(k-\nu)} iw_1\, dk = e^{iw_1\nu} \int_{l_-} \frac{e^{-iw_1 k}}{k-\nu}\, dk. \tag{5.3}$$

Let us now rewrite the integral over P_- as an integral on $-i\nu w_1 + \mathbb{R}_+$ by making use of the residue theorem. As seen on figure 5, there are two cases.

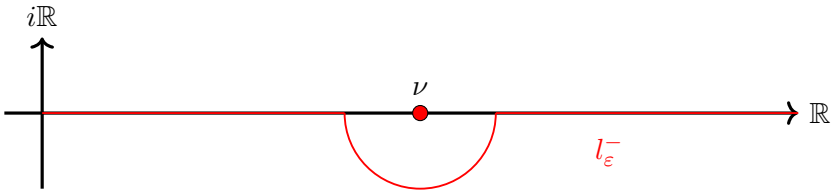

FIGURE 4. Path of integration for $k \mapsto \dfrac{e^{-ik(z-\bar{z}_1)}}{k-\nu}$

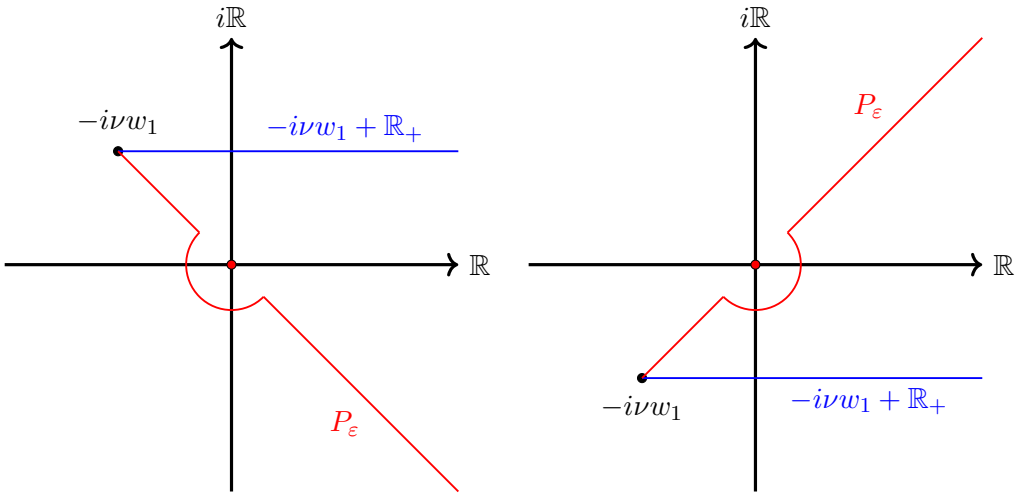

FIGURE 5. Paths of integration for $z \mapsto e^{-z}/z$ in (5.4) and (5.5). On the left: $\mathrm{Im}(-i\nu w_1 > 0)$, which means that $x < x_1$ (the point of observation z is upstream of the source z_1). On the right: $\mathrm{Im}(-i\nu w_1 < 0)$, which means that $x > x_1$ (the point of observation z is downstream of the source z_1).

If $(x - x_1) < 0$ (upstream, see figure 5, left), we close the path with an arc going from P_- to $-i\nu w_1 + \mathbb{R}$, and we use the decay at infinity for the positive real part of e^{-z}/z. Since the path encloses the singularity at $z = 0$, the residue theorem yields

$$\int_{P_-} \frac{e^{-z}}{z}\, dz = \int_{-i\nu w_1 + \mathbb{R}_+} \frac{e^{-z}}{z}\, dz + 2\pi i \mathrm{Res}(z \to \tfrac{e^{-z}}{z}, 0) = E_1(-i\nu w_1) + 2\pi i. \quad (5.4)$$

If $(x - x_1) > 0$ (upstream, see figure 5, right), by the same arguments, and noticing this time that the singularity is at the exterior of the path of integration, we have

$$\int_{P_-} \frac{e^{-z}}{z}\, dz = E_1(-i\nu w_1). \quad (5.5)$$

Summing up (5.2), (5.3), (5.4) and (5.5), we find

$$\begin{aligned}&\int_0^{+\infty} \frac{\cos(k(x-x_1))}{k-\nu} e^{k(y+y_1)} dk + \pi e^{\nu(y+y_1)} \sin(\nu(x-x_1)) \\ &= \begin{cases} \mathrm{Re}\{e^{-i\nu w_1}[E_1(-i\nu w_1) + 2\pi i]\} & \text{if } x < x_1, \\ \mathrm{Re}\{e^{-i\nu w_1} E_1(-i\nu w_1)\} & \text{if } x > x_1. \end{cases}\end{aligned} \tag{5.6}$$

In this way, the integral term in the Green's function (3.1) can be expressed as the real part of a holomorphic function involving E_1 (recall that the oscillating part $\sin(\nu(x-x_1))$ vanishes for the waveless potential $\Phi_{a,d,m}$).

For the numerical resolution, there are two other important remarks.

First, we note that it is possible to choose a stream function which is continuous on $\mathbb{R}^2_- \setminus [z_-, z_+]$. More precisely, we can set

$$\psi_2(x,y) = \psi(x,y) + \begin{cases} 2\pi & \text{if } -a < x < a \text{ and } y < -d, \\ 0 & \text{otherwise,} \end{cases} \tag{5.7}$$

where ψ is defined by (4.21). Analogously, we can choose a determination of the complex potential $\omega(z)$ which is holomorphic on $\{\mathrm{Im}\, z < d/2\} \setminus [z_-, z_+]$, by choosing appropriate branch cuts for the logarithmic function.

Second, we find the critical point z_b as the zero of $\omega'(z)$ by applying the numerical solver `fsolve` applied to the function $(z - z_+)\omega'(z)$ (cf. (4.8)); the starting point for the solver is z_+.

Once we have the critical point, the Rankine body is found as a subset of the streamline $\psi_2(x,y) = \psi_2(x_b, y_b)$ (with additional care if this streamline crosses the segment $[z_-, z_+]$ as in Figure 8, right).

5.2. **Numerical results.** In Figures 6-11, we present several Rankine bodies obtained for different values of the parameters. The source is in green and the sink is in magenta. The streamlines are represented in black. The streamline which contains the critical point appears in red, and so the boundary of Rankine body is the red Jordan curve contained in this streamline. Note that the red segment between the source and the sink is due to a discontinuity of the stream fonction (cf. (5.7)). *This segment should not be interpreted as a streamline in the figures.*

The parameters are $U_\infty = 1\ \mathrm{m\,s^{-1}}$, $g = 9.81\ \mathrm{m\,s^{-2}}$. The lengths are expressed in meters and the strength m of the source and sink is in $\mathrm{m^2\,s^{-1}}$. We have chosen $a = \pi/\nu$, except in Figure 10 where $a = 2\pi/\nu$ and Figure 11 were $a = 3\pi/\nu$. As is well-known, there is a scaling invariance in the Neumann-Kelvin problem, which consists in multiplying all the lengths by a dimensionless number α and the speed U_∞ by $\sqrt{\alpha}$. Thus, choosing a specific U_∞ does not restrict the generality of the simulations.

The first figure, Figure 6 (left) shows a Rankine body for a small m, namely $m = 0.05$. It is close to a Rankine body whose existence is asserted in Theorem 4.1. It represents an obstacle similar to a flat classical Rankine oval, with a small hollow on the upper side. As the strength m increases ($m = 0.3$, $m = 0.6$ and $m = 0.9$ in Figures 6 and 7), the area of the Rankine body increases and the hollow is more present. For m too large (for instance if $m \geq 1$ when $d = 0.2$), the potential no longer defines a Rankine body (the trajectory starting from the critical point does not reach the y axis).

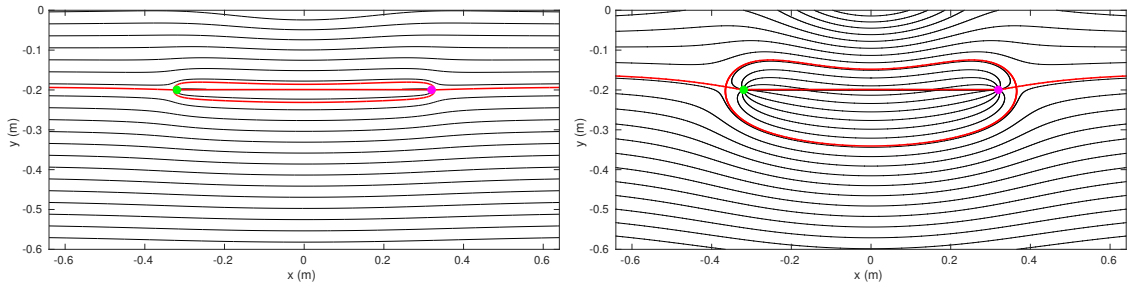

FIGURE 6. Rankine body for $d = 0.2$, $m = 0.05$ (left) and $m = 0.3$ (right)

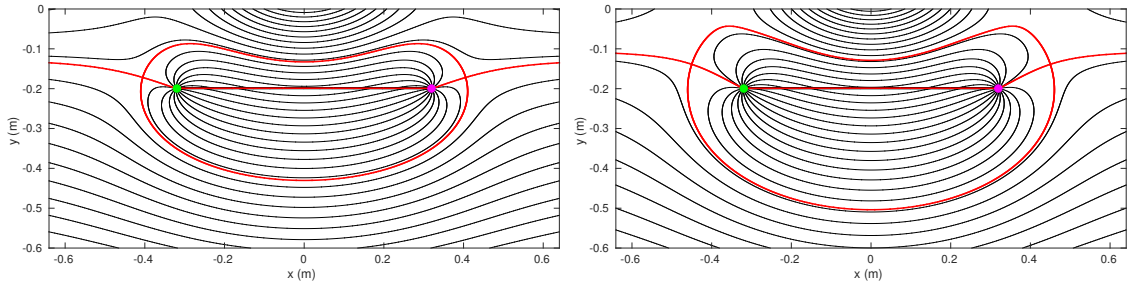

FIGURE 7. Rankine body for $d = 0.2$, $m = 0.6$ (left) and $m = 0.9$ (right)

For a given m, we observe that as the depth d increases, the influence of the "free" surface becomes negligible and the Rankine body converges to the classical Rankine oval. This can be seen by comparing Figure 8 (left) where $d = 0.4$ with Figure 7 (right) where $d = 0.2$, for the same m.

In Figure 8 (right), the depth is small and we have an example where the hollow of the Rankine body crosses the discontinuity segment $[z_-, z_+]$. We stress that the Rankine bodies that we build here are very similar to the shapes found numerically in [13] by a shape optimization approach.

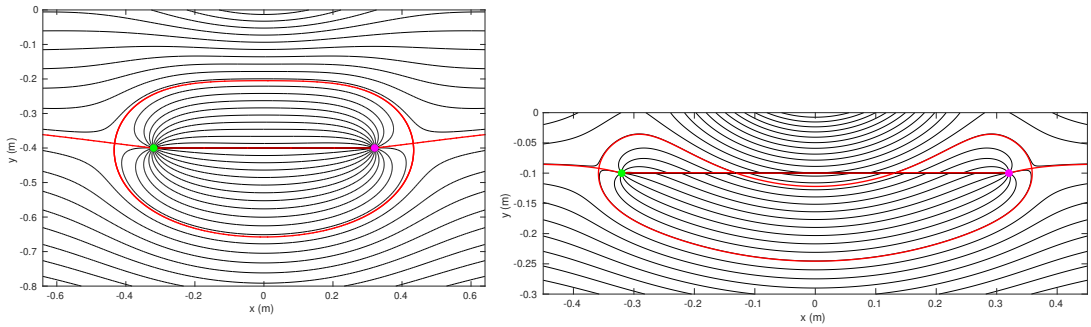

FIGURE 8. Cases $d = 0.4$, $m = 0.9$ (left) and $d = 0.1$, $m = 0.2$ (right)

In Figure 9, we show the Rankine body obtained for $a = \pi/\nu$, $d = 0.2$ and $m = 0.35$. The surface elevation is also represented (blue line). It can be recovered from the velocity potential $\Phi_{a,d,m}$ through $\eta(x) = -(U_\infty/g)(\partial_x \Phi_{a,d,m} - U_\infty)$ [7, 13] where $y = \eta(x)$ is the graph of the elevation function. We see that there is a bump

above the obstacle, followed by a hollow of smaller amplitude. The surface elevation is symmetric about the y axis and away from the obstacle, it tends to 0, as expected for a waveless potential.

In Figure 10, the parameters are the same as in Figure 9, except that $a = 2\pi/\nu$. That is, the length between the source and the sink is twice the prous one. The obstacle has two hollows on its upper side corresponding to two bumps in the surface elevation above the obstacle. Analogously, in Figure 11 where $a = 3\pi/\nu$, there are three bumps above the obstacle.

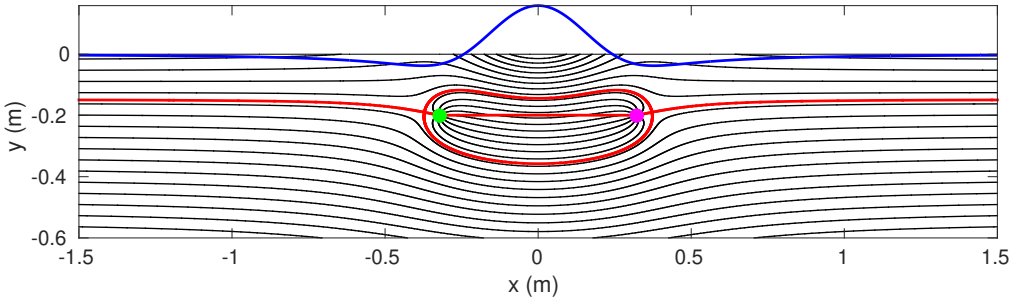

FIGURE 9. Rankine body with surface elevation for $a = \pi/\nu$, $d = 0.2$ and $m = 0.35$

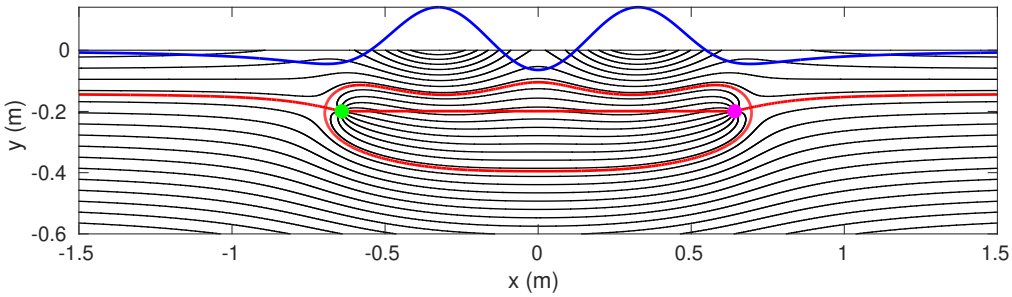

FIGURE 10. Case $a = 2\pi/\nu$, $d = 0.2$ and $m = 0.35$

ACKNOWLEDGEMENTS

The authors acknowledge the group "Phydromat" for stimulating discussions. Julien Dambrine wishes to thank the Wolfgang Pauli Institute (UMI CNRS 2842) for their support during this research. This work benefited from the support of the project OFHYS of the CNRS 80|prime 2019 initiative.

REFERENCES

[1] L. K. Forbes. On the wave resistance of a submerged semi-elliptical body. *J. Engrg. Math.*, 15(4):287–298, 1981.

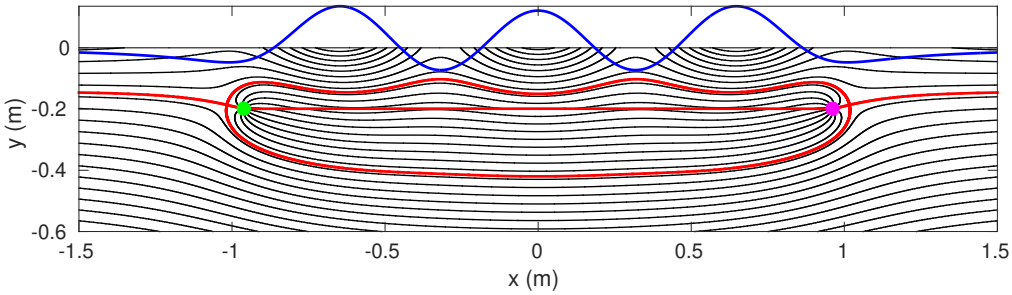

FIGURE 11. Case $a = 3\pi/\nu$, $d = 0.2$ and $m = 0.35$

[2] L. K. Forbes. Non-linear, drag-free flow over a submerged semi-elliptical body. *J. Engrg. Math.*, 16:171–180, 1982.
[3] A. Haraux. *Systèmes dynamiques dissipatifs et applications*, volume 17 of *Recherches en Mathématiques Appliquées*. Masson, Paris, 1991.
[4] J. He, Y. Zhu, C. Ma, C.-J. Yang, W. Li, and F. Noblesse. Boundary integral representations of steady flow around a ship. *Eur. J. Mech. B Fluids*, 72:152–163, 2018.
[5] A. Henrot and M. Pierre. Un problème inverse en formage des métaux liquides. *RAIRO Modél. Math. Anal. Numér.*, 23(1):155–177, 1989.
[6] A. A. Kostyukov. *Theory of ship waves and wave resistance*. Effective Communications Inc., Iowa City, Iowa, 1968.
[7] N. Kuznetsov, V. Maz'ya, and B. Vainberg. *Linear water waves*. Cambridge University Press, Cambridge, 2002.
[8] N. Kuznetsov and O. Motygin. On the waveless statement of the two-dimensional Neumann-Kelvin problem for a surface-piercing body. *IMA J. Appl. Math.*, 59(1):25–42, 1997.
[9] M. McIver. An example of non-uniqueness in the two-dimensional linear water wave problem. *J. Fluid Mech.*, 315:257–266, 1996.
[10] R. E. Meyer. *Introduction to mathematical fluid dynamics*. Wiley-Interscience, New York, 1971.
[11] O. V. Motygin and P. McIver. Non-uniqueness in the plane problem of steady forward motion of bodies. In *Proceedings of 25th Workshop on Water Waves and Floating Bodies*, pages 117–120, 2010.
[12] J. N. Newman. *Marine hydrodynamics, 40th anniversary edition*. MIT Press, 2018.
[13] E. Noviani. *Shape optimisation for the wave-making resistance of a submerged body*. PhD thesis, Université de Poitiers, 2018.
[14] J. V. Wehausen and E. V. Laitone. Surface waves. In C. Truesdell, editor, *Fluid Dynamics, Strömungsmechanik. Encyclopedia of Physics, Handbuch des Physik*, volume 3/9, pages 446–778. Springer, Berlin, Heidelberg, 1960.

LABORATOIRE DE MATHÉMATIQUES ET APPLICATIONS, UNIVERSITÉ DE POITIERS, CNRS, F-86073 POITIERS, FRANCE.